MULTIPLEXED PERMANENT AND REAL-TIME HOLOGRAPHIC RECORDING IN PHOTOREFRACTIVE BSO.

N. A. Vainos, S. L. Clapham[+] and R. W. Eason[+]

University of Essex

Department of Physics

Wivenhoe Park

Colchester CO4 3SQ, U.K.

[+]Present address: Department of Physics, The University, Highfield, Southampton SO9 5NH, U.K.

ABSTRACT

We report permanent hologram recording in crystals of photorefractive bismuth silicon oxide (BSO) using reversible photochromic effects. At a recording wavelength of 488 nm, exposures of several minutes produce areas of faint discolouration in which the permanent hologram is stored. The normal photorefractive behaviour is unaffected however, permitting spatial multiplexing of both real time and permanent holograms. Experimental results and characteristics of this permanent recording in combination with the photorefractive process are presented.

PACS Numbers

42.65, 42.40, 42.30

1.Introduction.

Bismuth Silicon Oxide (BSO) is a widely used photorefractive (PR) crystal that has found numerous applications in the fields of optical phase conjugation, real time holography and optical information processing [1]. While most of the interest in BSO and other photorefractives stems from its real time recording characteristics, there are also areas where permanent or controlled semi-permanent storage is also required. Obvious examples of this would lie in the fields of optical storage, interferometry and vibration analysis techniques [2] and also perhaps spatial light modulator devices.

Fixing processes that have achieved either permanent or at least fairly long-term storage have been reported for photorefractive materials using a variety of techniques [3,4]. In BSO, a room temperature technique has recently been demonstrated [5] that involves charge compensation via hole conduction allowing a 40-fold increase in storage time. There are however to our knowledge no reports of fixing processes or techniques for permanent storage, that are not only very simple but also allow the simultaneous storage of permanent and real time holograms within the same crystal volume. In this paper we report such a scheme that allows normal photorefractive real-time behaviour in addition to a permanent recording mechanism which is attributable to photochromic behaviour.

Reversible photochromic effects have been observed before in

doped BSO, and in BGO (Bismuth Germanium Oxide) [6]. While photochromic properties in BSO have been formerly regarded as a problem rather than a possible mechanism for holographic storage [7], the use of BSO and BGO for permanent photographic and holographic recording was only suggested in [6]. This photochromic recording has not been investigated before, to our knowledge, although holograms have been successfully recorded in other photochromic materials in the past [8]. We present here the characteristics of photochromic hologram formation in BSO including certain dynamic processes observed. These processes involve the enhancement of the diffraction efficiency of the permanent hologram on its illumination by additional beams. The application of an external electric field also results in the variation of the diffraction efficiency and the interferometrically observed phase shift of the permanent hologram.

2. Experimental results and discussion.

Fig. 1. shows the experimental arrangement used to investigate the formation of permanent holograms. In this typical write-read configuration, beams 1 and 3 record the hologram in the crystal and readout is performed by beam 2. For these experiments three different BSO crystals were used. Crystal A ($9\times10\times2mm^3$) was obtained from GEC, while crystal B ($8\times8\times2mm^3$) and C ($9\times10\times3mm^3$) were obtained from Crystal Scintillators. The crystals were mounted on a stand allowing controlled rotation and horizontal displacement.

The photorefractive (real-time) and photochromic (permanent) holograms were written using an argon ion laser operating in multilongitudinal mode at λ=488nm and at typical intensities for beams 1 and 3 of $I_1=I_3=1.4$ Wcm^{-2}. The measured transmission of crystals A, B and C (excluding Fresnel losses) at λ=488nm were 29%, 22% and 14% respectively. The angle 2ϑ between writing beams 1 and 3 was varied between 2 deg. and 30 deg. for the different holograms recorded.

Readout was performed by using a He-Ne laser at 633nm (≃5mW), which was incident on the BSO at the angle for maximum Bragg scattering efficiency. Diffracted beam 4 was monitored by a Spectra-Physics power meter, D1, filtered by a 633nm interference filter, IF, to minimise the effects of stray light. The output of D1, the combined diffraction efficiency (η_T) of the permanent and real-time holograms was monitored by using a y-t chart recorder.

Photodiode D2 monitored the undiffracted He-Ne beam as a witness for the possible effects of photochromic absorption. A constant increase in absorption was evident. Shutter SH1 was used to switch off the writing beams at regular intervals in order that the diffraction efficiency of the permanent hologram (η_{PC}) only was recorded. Shutter SH2 was used to switch off writing beam 1 at arbitrary intervals to monitor the diffraction efficiency (η'_{PC}) of the permanent hologram in the presence of beam 3 only.

Hologram exposure times were in the range of 5 minutes to more than 300 minutes and it should be noted that recording was

possible at all the green-blue argon-ion laser wavelengths available. For the longer wavelengths however, longer exposures were required for efficient recording. To verify the reversible nature of this permanent recording, all three crystals were indirectly heated in silicone oil at temperatures ranging from 100°C to 200°C. At 150°C all the photochromic discolouration was erased in a time of about 1 hour. A qualitative estimate indicated that, as expected, erasure proceeds faster at higher temperatures. Fig. 2 shows a picture of one of the crystals, in which the darker regions are areas where permanent holograms have been stored.

Fig. 3. shows typical traces of diffraction efficiency, η, (uncorrected for losses) as a function of time recorded on the y-t time and permanent holograms (η_T) which are spatially multiplexed in the same crystal volume. The Bragg angle was θ=1.25 deg. in this case. When shutter SH1 was closed, blocking beams 1 and 3, the diffraction efficiency, $_{PC}$, of the permanent hologram was sampled for a period of ~4 sec. Curve (c) shows the development of this permanent hologram with time, indicating that, after a long period of time, the diffraction efficiency approaches saturation. A steady increase in the difference of diffraction efficiencies between permanent, (c), and permanent/real-time, (a), is observed. This result is expected since the real-time and permanent holograms are essentially independent and the permanent (absorption) grating is expected to be unshifted with respect to the interference pattern, while the real-time grating, in the diffusion regime, is $\pi/2$-shifted. Therefore, the resulting $\pm\pi/2$ spatial shift between the multiplexed gratings combined with the

scattering processes should result in the coherent addition (depending on crystal orientation) between the scattered fields as it is observed. The unexpected effect here is the increase of the diffraction efficiency η_{PC} on illumination of the recording region by an additional beam. To investigate this behaviour, we monitored the diffraction efficiency η'_{PC} with only one writing beam present by using shutter SH2 (curve (b)). A much higher diffraction efficiency is observed in this case. The difference in diffraction efficiency between curves (a) and (b) remains nearly constant and is about equal to the initial diffraction efficiency of the real-time grating alone, i.e., before the formation of the permanent hologram.

The alternative possibility of destructive interference between the fields scattered by the stored permanent and a phase-shifted stored PR grating has also been investigated by erasing the PR grating. An additional beam, 5, at 488nm was used to simulate the conditions of having one of the writing beams on (Fig. 1), after the formation of a permanent hologram. Indeed, while the PR grating is naturally erased (here in ~2 sec) with the presence of beam 5, an increased diffraction efficiency of the permanent hologram is observed. However, when the writing beam (or beam 5) is continuously on, the contrast of the permanent grating decreases, over a fairly long time scale, due to the uniform illumination, i.e., the crystal becomes uniformly dark and the diffraction efficiency falls to zero.

Fig. 4 shows a typical experimental plot of this increased diffraction efficiency of the permanent hologram as a function of intensity (uncorrected for Fresnel losses) of the enhancing beam 5. In this case we observe that only $\simeq$ 2 $mWcm^{-2}$ at 488nm is enough to produce a six-fold increase in diffraction efficiency. This enhancement process is very fast with an intensity dependent rise-time in the millisecond time scale. An experimental plot of the rise time (90% of max. value), τ_r, as a function of the intensity of beam 5 is shown in Fig. 5. The insert depicts a typical oscilloscope trace of the output beam 4 on chopping beam 5. A longer relaxation (intensity independent) time, τ_f, is always observed.

Fig. 6. depicts the long-term development of combined real time and permanent holograms in the crystal as a function of time. An oscillatory behaviour is observed in nearly all cases. With reference to Fig. 6(i), development of the real-time grating occurs typically some milliseconds after the shutter SH1 is opened. The formation of the permanent hologram starts at the same time and their combined diffraction efficiency decreases after some minutes, possibly due to the increased absorption in the crystal (region A in figure). After this initial dip which is always observed, both η_T and η_{PC} steadily increase. It is always observed that during the period of permanent hologram formation the output appears to be relatively stable, as indicated by the nearly vibration-free trace in region B (see also curve (a) in Fig. 3). Close to the saturation region C, larger vibrations begin to develop spontaneously. After a certain period of time the

vibrations become stronger and η_T rapidly decreases. The diffraction efficiency of the permanent hologram with (curve (b)) and without (curve (c)) the presence of one writing beam also decreases. After the region of decrease, the total diffraction efficiency increases again and the trend appears to repeat itself. The diffraction efficiency of the second maximum however, may be lower than the first maximum and we have observed slightly different behaviour in the recordings depicted (e.g. Fig. 6(ii),(iii)). Even if recording was stopped for a long period of time, the recorded pattern would always start again at the point of interruption. Generally though, in all recordings the diffraction efficiency, η_{PC}, appears independent of the Bragg angle but very dependent on the exact region of the crystal used for hologram formation. This is probably due to the non-uniform crystal properties (e.g. density of defects) induced during crystal growth. Such effects may obscure any angular dependence. Two distinct cases are shown in Fig. 6(ii) and 6(iii). We have also to note here that the observed minima in η_T and η_{PC} do not occur simultaneously as the apparent shift indicates and also that at this minima the combined diffraction efficiency is lower than the initial real-time hologram diffraction efficiency (before the permanent hologram formation) i.e., the normal PR processes seem to be suppressed.

In addition, we have investigated the behaviour of the permanent holograms in the presence of externally applied high electric fields. Experimentally, we formed a hologram using the

arrangement of Fig. 1 and used the technique of photoconductive enhancement [9] to apply the electric fields. In this technique, an additional beam at 488 nm is used to uniformly illuminate the crystal thereby transferring the voltage from the electrodes to the region of the hologram via photoconduction. This technique was employed firstly because unexpanded beams were used for hologram recording and, secondly, in order to create extremely high electric fields in the region of interest.

The first effect observed here was a variation in diffraction efficiency of the hologram in a manner similar to that observed for photorefractive behaviour. This variation was seen to be dependent on the intensity of beam 5 in the region of the permanent grating and also on the direction of the electric field in the crystal (voltage polarity). The second effect observed was an interferometrically detected phase shift of the permanent hologram with the application of an electric field. The beam diffracted by the permanent hologram was recombined with a reference beam at a beam splitter (arrangement not shown in Fig. 1) and the output was detected by a TV camera. At a maximum applied field of about 18 kV/cm, a phase shift of about 4π was detected. For the photorefractive grating however, a much smaller phase shift, of between 0 and $\pi/2$, was observed on the application of an electric field of the same magnitude, entirely as expected [1]. We have to note here that, in addition to the shift of the grating, there is a contribution due to the electro-optically and piezo-electrically induced variation of the optical path length in the bulk crystal volume occuring as a result of the applied field.

These latter effects however, are limited firstly by the dynamic range of the material and, secondly, are expected to contribute equally in both cases examined (real-time and permanent).

If we consider, in general, the behaviour of permanent absorption gratings, then there are several unexpected effects observed in the present case of permanent holograms in BSO. These are (i) the enhancement of the diffraction efficiency of the permanent hologram by an additional beam, (ii) the variation of the diffraction efficiency and phase shift of the grating by an applied electric field, and (iii) effects observed during the long-term development of the permanent hologram.

As we mentioned before, the photochromic effects observed in [6] and [7] are due to the reduction of Mn and oxidization of Cr impurity centres. To our knowledge, natural defects which may be formed during crystal growth may also contribute to the photochromic behaviour. Uniform illumination of the hologram by the beam at 488 nm creates photocarriers (mainly electrons). The trapping of these carriers at neighbouring photochromic sites used for hologram recording results possibly in increased absorption and therefore in the enhancement of the diffraction efficiency. The alternative effect of excitation of carriers from photochromic centres is also a possibility. The high speed of this process indicates that the effect is localised. The variation of the diffraction efficiency with voltage may be the result of the drift of charge and consequent recombination.

The origin of the phase shifting behaviour, as well as all the effects observed, is not well understood and we are currently investigating the various mechanisms responsible. Nevertheless, we have demonstrated several applications based upon the present scheme of multiplexing two distinct holographic gratings. These techniques range from optical switching and image synthesis to holographic interferometry, and results will appear in a following publication.

3. Conclusions.

Bismuth silicon oxide crystals have shown discolouration under intense illumination at the green-blue wavelengths due to absorption by impurity centers. This effect has been used for the formation of permanent (absorption) holograms in this material. The combination of real-time and permanent holographic recording has been investigated and the development of the multiplexed real-time and permanent holograms has been presented.

An oscillatory variation of the diffraction efficiency of both holograms has been observed during long-term recording of the permanent hologram. Other significant and unexpected effects observed here are the increase of the diffraction efficiency of the permanent hologram upon illumination of the grating by a beam at the highly absorbed blue wavelengths, the variation of this diffraction efficiency and the phase shift of the permanent grating on the application of external electric fields.

Acknowledgements.

The authors are grateful to the ´M. Kassimati´ Foundation, Greece, for a scholarship for N.A.V. and to the Science and Engineering Research Council for a CASE studentship for S.L.C..

REFERENCES

[1] P. Gunter, "Holography, coherent light amplification and optical phase conjugation with photorefractive materials.", Phys. Rep., 93, 199(1982)

[2] J. P. Huignard, J. P. Herriau and T.Valentin,"Time average holographic interferometry with photoconductive electrooptic $Bi_{12}SiO_{20}$ crystals", Appl. Opt., 16,2796(1977)

[3] G. R. Knight in "Optical Information Processing", S.H. Lee ed., Springer-Verlag, New York (1981).

[4] F. Micheron and G. Bismuth, "Electrical control of fixation and erasure of holographic patterns in ferroelectric materials", Appl. Phys. Lett., 20, 79(1971)

[5] J. P. Herriau and J. P. Huignard, "Hologram fixing process at room temperature in photorefractive $Bi_{12}SiO_{20}$ crystals." Appl. Phys. Lett., 49, 1140(1986)

[6] W. Wardzynski, T. Lukasiewicz and J. Zmija, "Reversible photochromic effects in doped single crystals of bismuth germanium ($Bi_{12}SiO_{20}$) and bismuth silicon ($Bi_{12}SiO_{20}$) oxide.", Opt. Commun., 30, 203(1979)

[7] A.R. Tanguay, Jr., S. Mroczkowski and R.C. Barker, "The Czochralski growth of optical quality bismuth silicon oxide ($Bi_{12}SiO_{20}$).", J. Crystal Growth, 42, 431(1977)

[8] D.R. Bosomworth and H.J. Gerritsen, "Thick holograms in photochromic materials.", Appl. Opt., 7, 95(1968)

[9] R.W. Eason and N.A. Vainos, "Photoconductive enhancement of degenerate four-wave mixing reflectivity in BSO", J. Mod. Opt., 35, 491(1988)

FIGURE CAPTIONS

Fig. 1. Schematic of the experimental arrangement used. SF= spatial filter, IF=He-Ne interference filter, SH1,SH2= mechanical shutters, BS=R/T 50/50 beam splitter, D1, D2= calibrated photodiodes connected to the 2y-t chart recorder. An external voltage (0-6kV) was applied on the BSO via Au/Cr electrodes.

Fig. 2. Pictures of one of the BSO crystals used before, (a), and after, (b), the recording of the permanent holograms. The dark regions are areas where holograms are permanently stored.

Fig. 3. Recorded diffraction efficiency of (a) the combined permanent and real-time (PR) holograms, η_T; (b) the permanent hologram in the presence of one of the writing beams, η'_{PC}, and (c) the permanent hologram only, η_{PC}, as a function of exposure time.

Fig. 4. Typical diffraction efficiency of the permanent hologram as a function of the enhancing beam (488 nm), I_5. The arrow indicates the initial (unenhanced) diffraction efficiency.

Fig. 5. Rise time, τ_r, of the enhancement process as a function of the intensity of the enhancing beam, I_5. The insert shows a typical oscilloscope trace of the diffracted beam.

Fig. 6. Behaviour of long-term holographic recording for three different experimental runs ((i), (ii) and (iii)) for ϑ=8.5 deg.. Curve (a) is the diffraction efficiency of the combination of permanent and real-time holograms, η_T, curve (b) is the enhanced diffraction efficiency of the permanent hologram, η'_{PC}, and curve (c) is the diffraction efficiency of the permanent hologram alone, η_{PC}, as functions of time. The arrows indicate the diffraction efficiency of the real-time hologram before the formation of the permanent one.

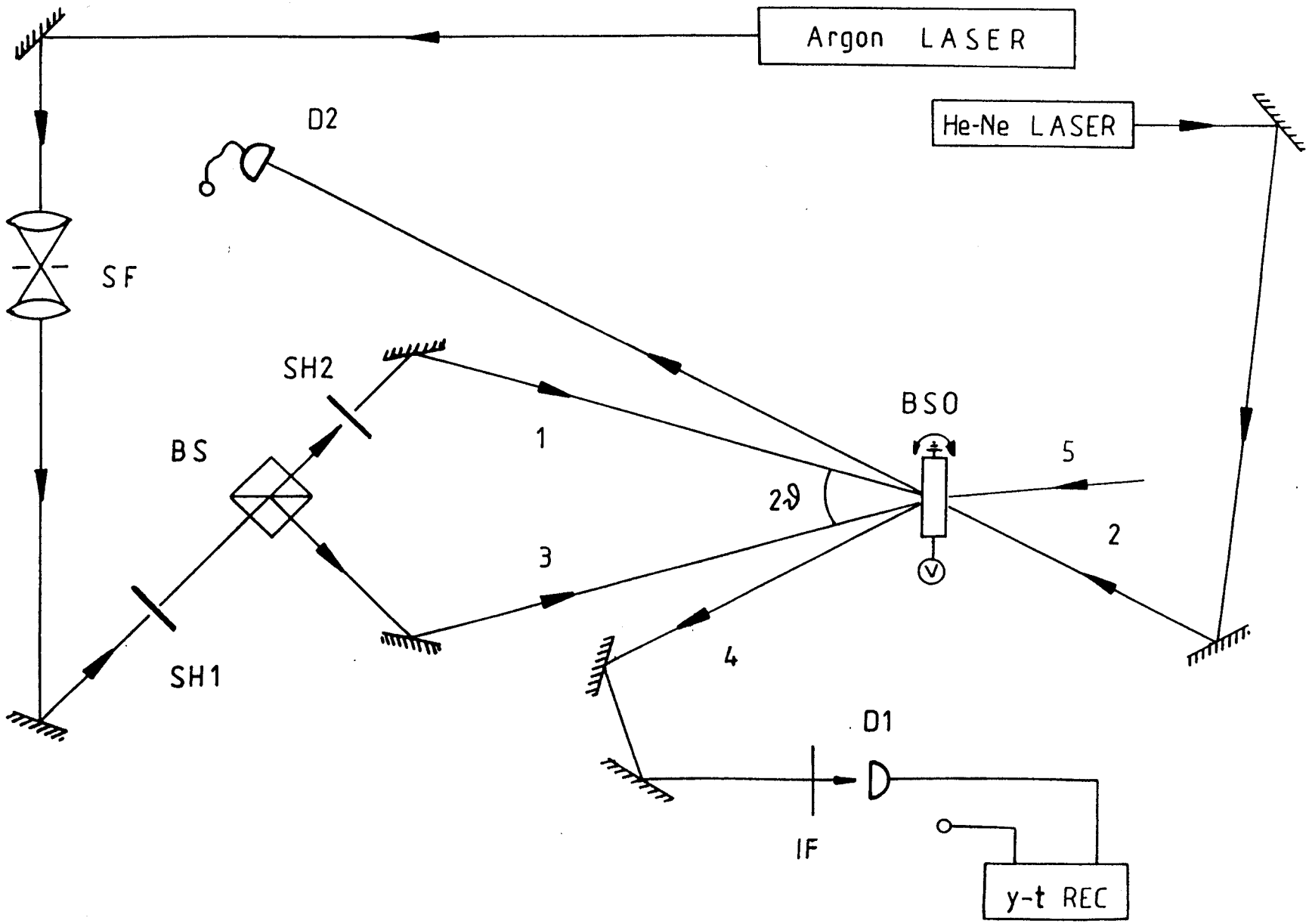
Argon LASER
He-Ne LASER
D2
SF
SH2
BS
BSO
1
5
2ϑ
2
3
SH1
4
D1
IF
D
y-t REC

Fig. 1

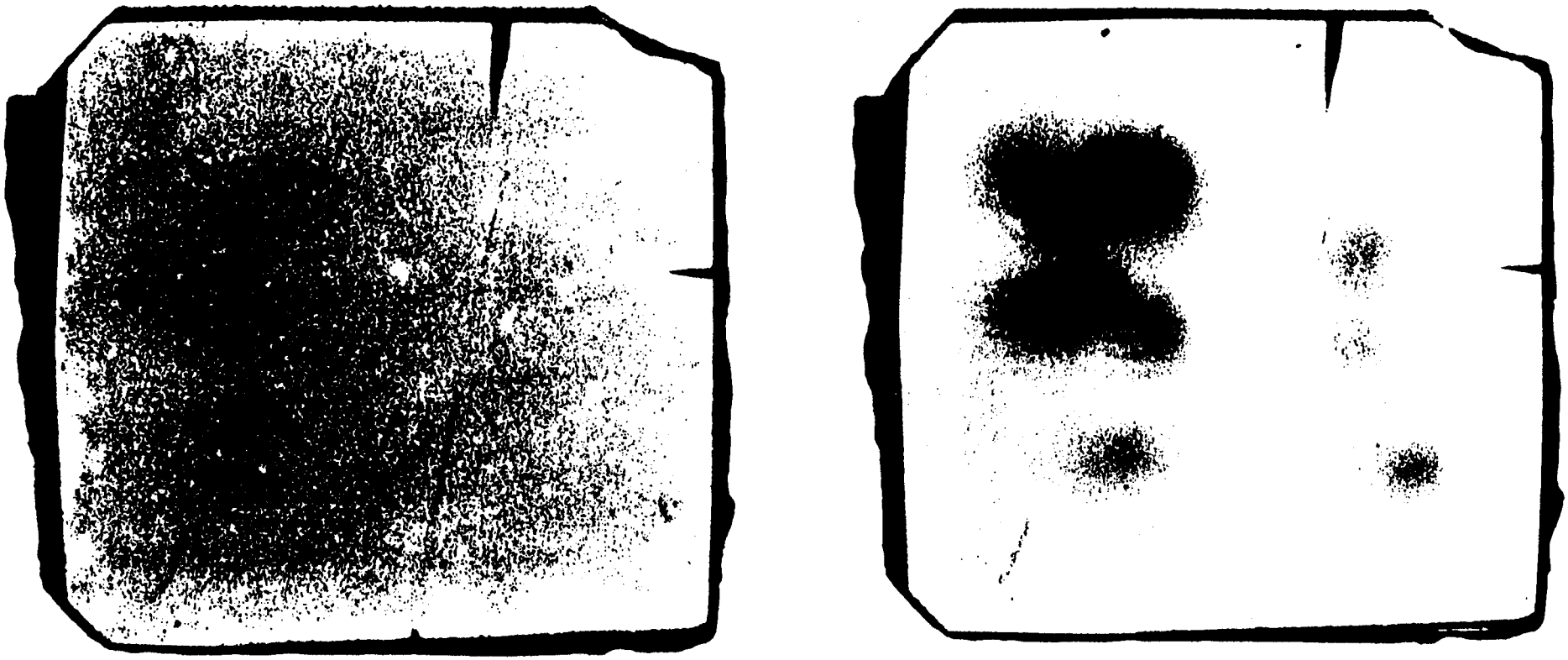

(a) (b)

Fig. 2

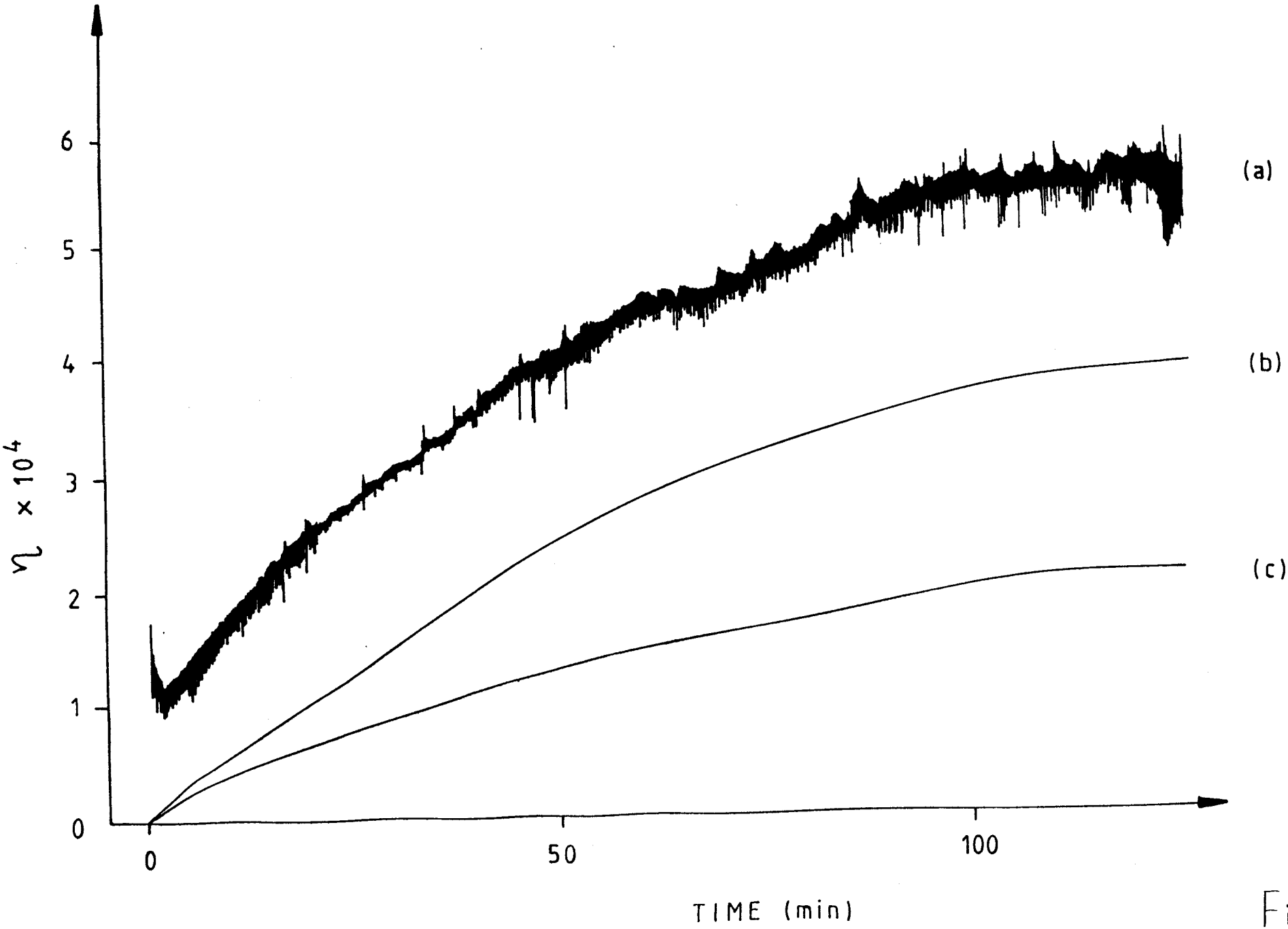

Fig. 3

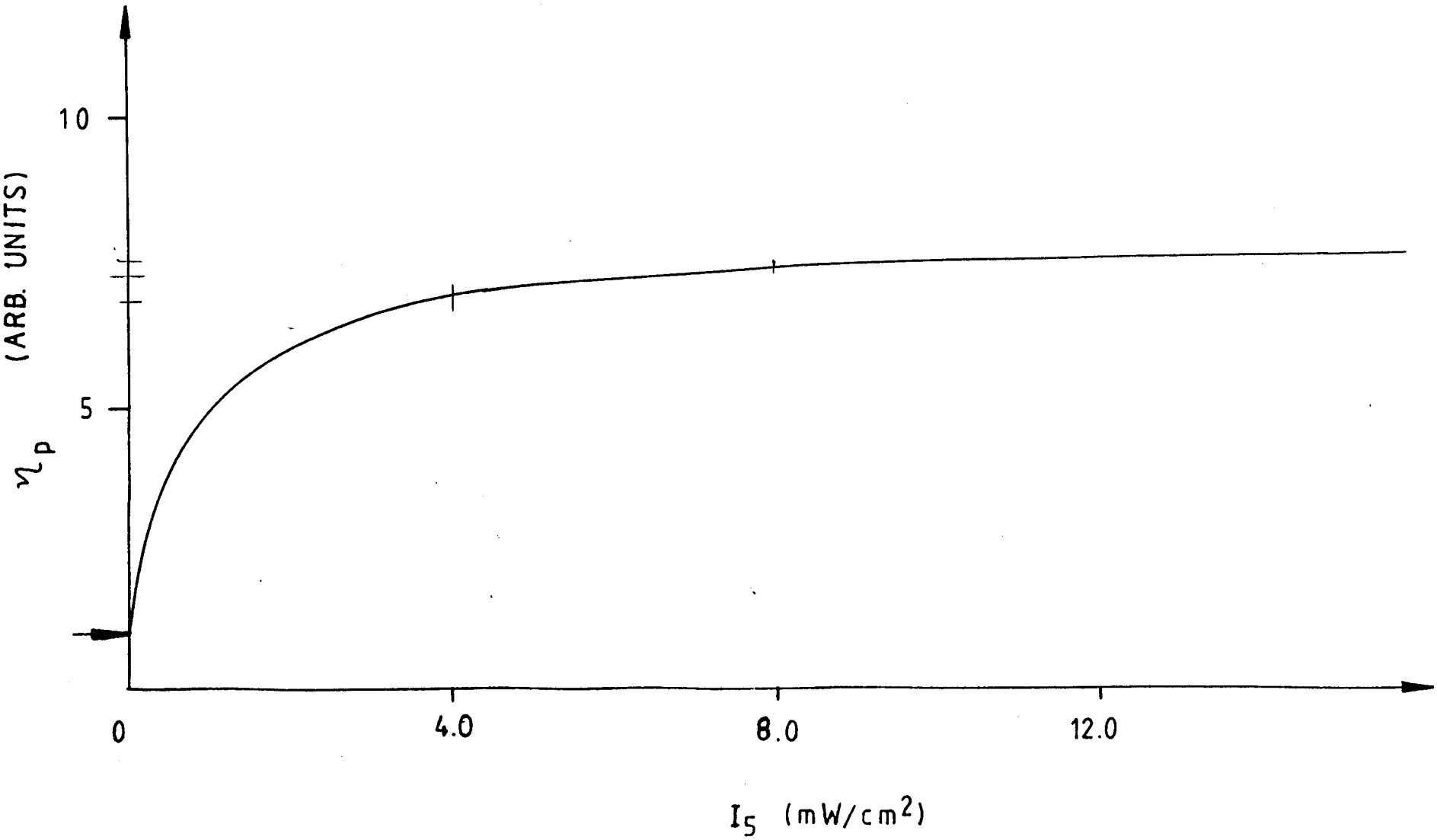

Fig. 4

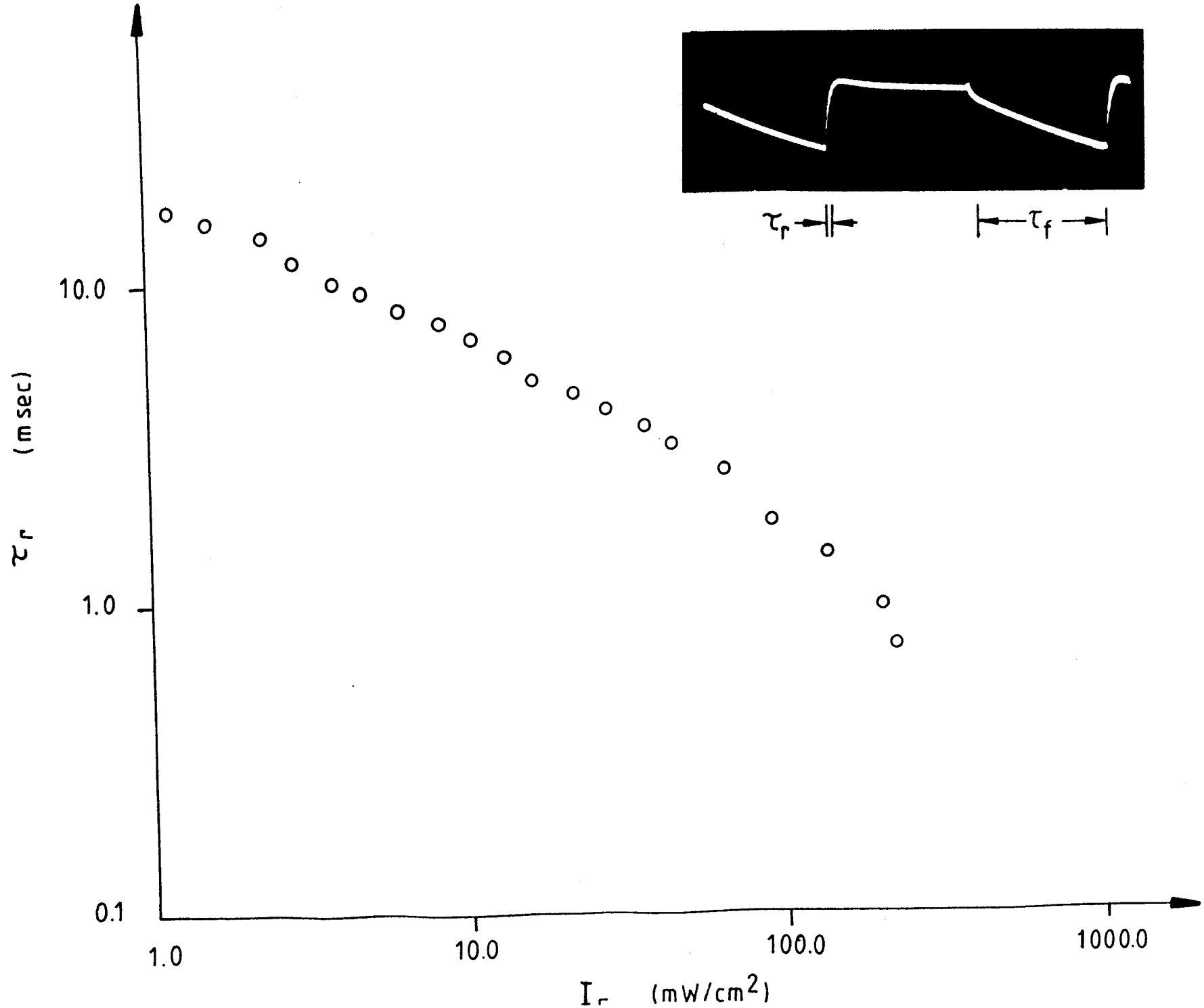

Fig. 5

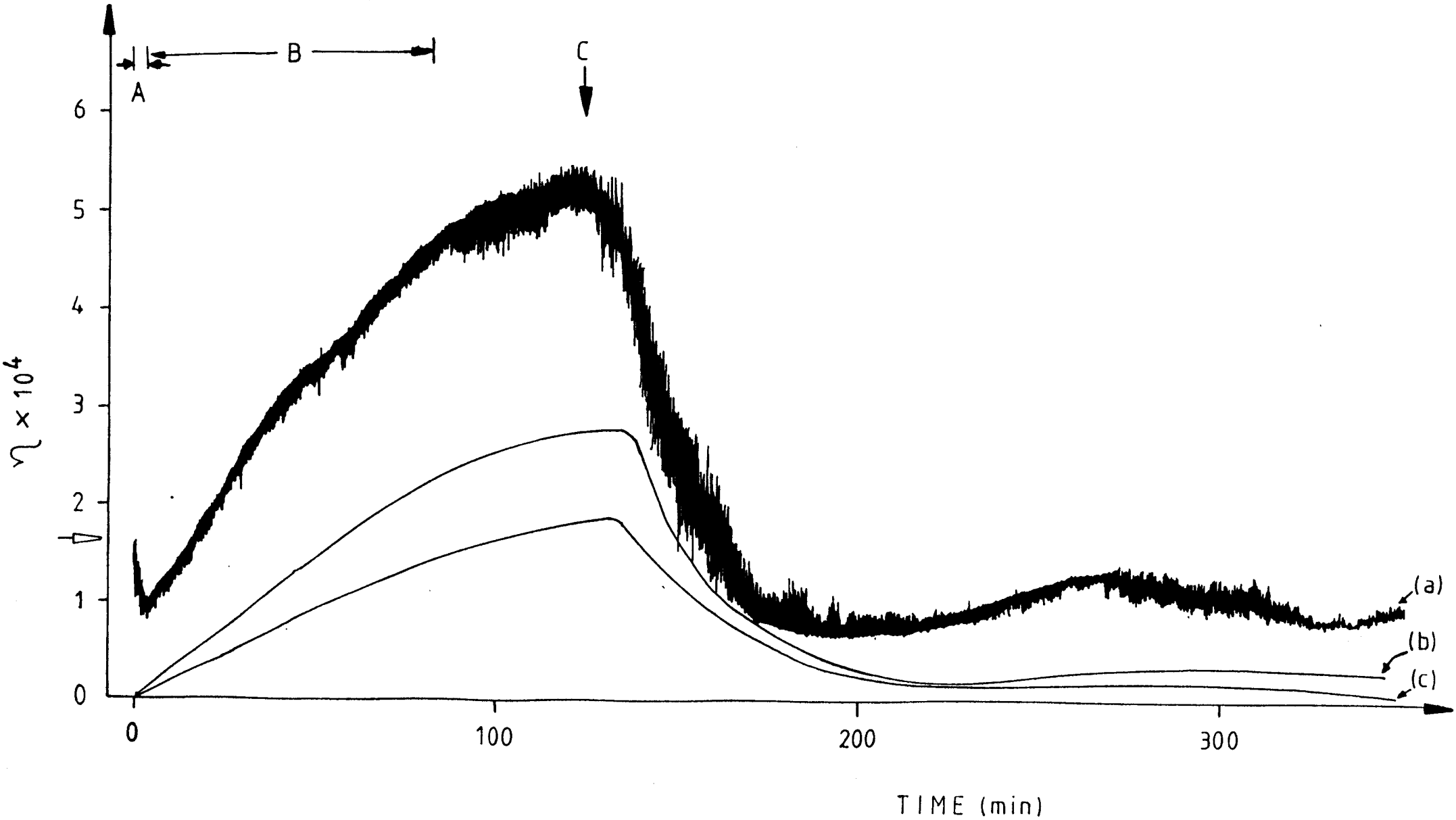

Fig. 6(i)

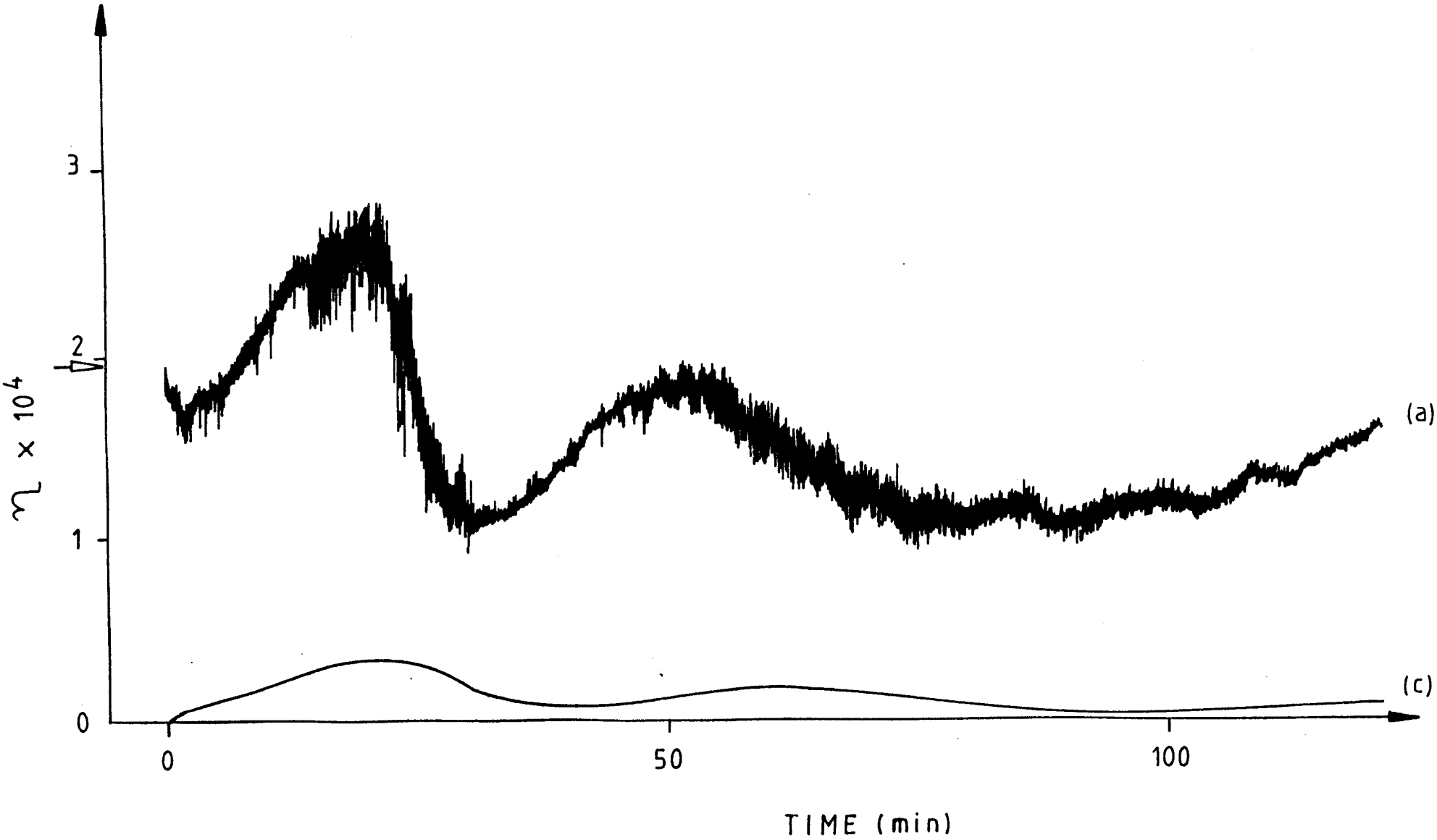

Fig. 6 (ii)

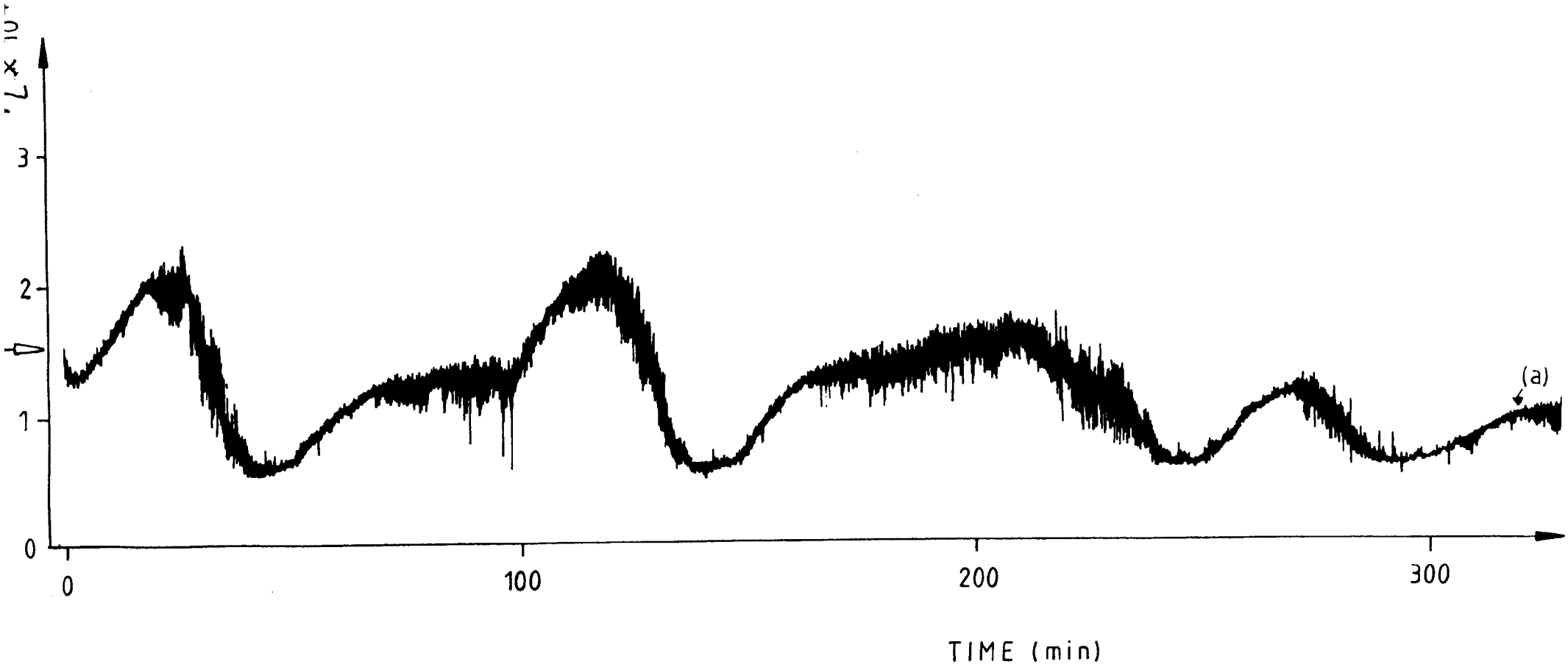

Fig. 6(iii)